Chem. Senses 33: 779–792, 2008
doi:10.1093/chemse/bjn041
Advance Access publication July 16, 2008

Comparison of Identified Mitral and Tufted Cells in Freely Breathing Rats: I. Conduction Velocity and Spontaneous Activity

Edwin R. Griff[1,2], Mariam Mafhouz[3], Anne Perrut[3] and Michel A. Chaput[2]

[1]Department of Biological Sciences, University of Cincinnati, Cincinnati, OH 45221-0006, USA, [2]Laboratoire de Neurosciences et Systèmes Sensoriels, Centre National de la Recherche Scientifique, UMR 5020, Université Claude Bernard Lyon 1, 50 Avenue Tony Garnier, 69366, Lyon, France and [3]Institut Camille Jordan, Equipe Probabilités et Statistiques, UMR 5208, Université Claude Bernard Lyon 1, 43 Bd du 11 Novembre 1918, Lyon-Villeurbanne, France

Correspondence to be sent to: Edwin R. Griff, Department of Biological Sciences, University of Cincinnati, ML 0006, Cincinnati, OH 45221-0006, USA. e-mail: edwin.griff@uc.edu

Abstract

The spontaneous activity and impulse conduction velocities of mitral and tufted cells were compared in the entire main olfactory bulb of freely breathing, anesthetized rats. Single units in the mitral cell body layer (MCL) and external plexiform layer (EPL) were identified by antidromic activation from the lateral olfactory tract (LOT), electrode track reconstructions based on dye marking, and the waveform of LOT-evoked field potentials. Using the track reconstructions, EPL units were further subdivided into glomerular border (GB) and not at the glomerular border (notGB) cells. For conduction velocity, significant differences were only found between MCL and GB units and not between MCL and all EPL units or between MCL and notGB units. For spontaneous activity, no significant differences were found between the different unit groups regarding the mean, maximum, or relative maximum rate per 100-ms bin. By contrast, they showed a differential modulation of their firing activity by respiration. GB but not notGB units had a significantly higher mean rate during the respiratory cycle than MCL units with significantly more activity during inspiration. Thus, mitral and tufted cells are similar in their impulse conduction velocity and spontaneous activity, though the more superficially placed GB cells exhibit differences. A comparison of odor responses in these cell types in the companion paper also points to differences between mitral and superficial projection tufted cells.

Key words: antidromic activation, main olfactory bulb, mitral cells, olfaction, respiration cycle, tufted cells

Introduction

For many sensory modalities, distinct subtypes of output neurons generally contained in the same structure process different aspects of the stimulus (somatosensory: e.g., Stewards TV and Stewards M 2002; auditory: e.g., Cant and Benson 2003; visual e.g., Schiller 1996). Such parallel processing is well documented, except in olfaction, where the role of the 2 populations of second-order neurons contained in the main olfactory bulb (MOB) remains unclear. Indeed, the mammalian MOB contains 2 populations of second-order neurons: 1) mitral cells, whose somata lie in a well-defined lamina called the mitral cell body layer (MCL), and 2) tufted cells, whose somata are scattered more superficially within the deep, intermediate and superficial sublayers of the external plexiform layer (EPL) and the deep part of the glomerular layer (Macrides and Schneider 1982; Orona et al. 1984; Mouradian and Scott 1988). These 2 classes of relay neurons share many anatomical and physiological features. Both cell types have a primary (apical) dendrite which terminates in an elaborate arborization within an olfactory glomerulus (Cajal 1911), where it receives excitatory glutamatergic input from olfactory receptor neurons (Berkowicz et al. 1994; Ennis et al. 1996) and juxtaglomerular interneurons (e.g., Wachowiak and Shipley 2006). Both types also exhibit dendrodendritic inhibition between their secondary (basal) dendrites and inhibitory granule cells (e.g., Orona et al. 1984; Christie et al. 2001). As relay neurons, both have axons that leave the MOB and project to the olfactory cortex via the olfactory tract (e.g., Haberly and Price 1977).

Several differences between mitral and tufted cells also have been reported regarding mainly the distribution of their secondary dendrites and axons and their responsiveness to electrical stimulation of the olfactory nerves (see review in Macrides et al. 1985). For example, the secondary dendrites of mitral cells ramify primarily in the deeper part of the EPL

where they can interact with type I and type II granule cells, whereas the secondary dendrites of middle tufted cells ramify more superficially in the EPL and may interact with type I and type III granule cells (Mori et al. 1983; Orona et al. 1984). Mitral cells are less responsive than tufted cells to orthodromic activation (Schneider and Scott 1983), and only mitral cells can be activated antidromically by electrical stimulation of the posterior piriform cortex (Scott 1981). Lastly, in rabbit, the conduction velocity of mitral cells is considerably faster than that of tufted cells (Nicoll 1970).

The tufted cells themselves do not form a homogeneous population (see review in Macrides et al. 1985). They were classified into 3 types—internal, medial, and external—by Cajal (1911), according to the laminar positions of their somata in the inner and external parts of the EPL and in the glomerular region. External tufted cells were shown to exhibit some characteristics that differentiate them from both mitral and other tufted cells (Macrides et al. 1985; Hayar et al. 2004; Kosaka K and Kosaka T 2005). For example, their dendritic arborization is more limited than the dendritic arborization of mitral and internal tufted cells (Pinching and Powell 1971), as is the spatial extent of lateral inhibition (Christie et al. 2001). Lastly, as mitral cells do, internal tufted cells may interact with granule cells that are morphologically and pharmacologically distinct from those that interact with external tufted cells (Macrides et al. 1985).

Ezeh et al. (1993) found it more convenient to deal with 3 groups of tufted cells: internal, intermediate, and superficial (Macrides and Schneider 1982; Scott and Harrison 1987), which were defined by the location of their basal dendrites in the EPL. They avoided use of the term "external tufted cell" because there are tufted cells in the periglomerular region so named that do not have long basal dendrites and are probably not output cells (Macrides et al. 1985). The internal tufted cells have the largest extraglomerular dendritic fields, similar to the dendritic fields of mitral cell. The secondary dendrites of progressively more superficially situated tufted cells showed a progressively smaller extension and a continuous trend toward spatial asymmetry in their tangential distributions with respect to the parent somata. Many of the tufted cells of the periglomerular region were reported to lack basal dendrites or have only short bushy basal dendrites (Pinching and Powell 1971; Macrides and Schneider 1982).

Tufted cells were also reported to differ in their projection patterns. Internal, middle, and at least a few tufted cells in the periglomerular region project to the rostral piriform cortex, but only internal tufted cells project to the posterior piriform cortex (Haberly and Price 1977). These tufted cells in the periglomerular region would have been classified as external tufted cells by Cajal (1911); thus, external tufted cells are a heterogeneous group.

Among the numerous electrophysiological studies performed on mitral and tufted cells, only a single one has analyzed the spontaneous activity and the odor-evoked responses of identified mitral and tufted cells in intact animals (Nagayama et al. 2004). Others were performed on MOB slices (e.g., Hayar et al. 2004; Antal et al. 2006), on cells identified by their position in the MOB, but recorded in tracheotomized animals (Onoda and Mori 1980), on cells referred to indistinctly as mitral/tufted cells recorded in or near the MCL in tracheotomized (Macrides and Chorover 1972) or freely breathing animals (e.g., Chaput and Holley 1979, Chaput et al. 1992), or on identified mitral and tufted cells responding to electrical stimulation of the olfactory nerve and/or olfactory tract in tracheotomized animals (Scott 1981; Schneider and Scott 1983; Doving 1987; Ezeh et al. 1993). The goal of this paper and its companion paper on responses to odors was to compare the electrophysiology of mitral and tufted cells in freely breathing animal. In these papers, all cells were identified as output neurons projecting from the MOB and cell activities were analyzed with reference to the respiratory cycle (Chaput and Holley 1979; Chaput et al. 1992). They differ from Nagayama et al. (2004) in that we recorded from antidromically driven cells throughout the MOB, and spike activity was analyzed as a function of the respiratory cycle. Furthermore, the overall conclusion differs: we found no differences between mitral and internal or middle tufted cells in most parameters measured for spontaneous activity. Differences were only found between mitral cells and tufted cells recorded at the level of the glomerular border (GB cells) of the EPL.

Materials and methods

Experiments were carried out in accordance with the European Communities Council Directive of 24 November 1986 (86/609/EEC) for the care and use of laboratory animals, and all efforts were made to minimize animal suffering and to reduce the number of animals used. Experimental protocols were approved by the Comité d'Expérimentation Animale de l'Université Claude Bernard—Lyon1.

General surgical techniques

The experiments were performed on 25 male Wistar rats, with a mean weight of 380 ± 40 g (range 260–430 g), purchased from Charles River Laboratories (Saint Germain sur l'Arbresle, France). Rats were housed individually at a temperature of 22 °C and 50% relative humidity under a normal 12:12 h light:dark cycle (lights on at 10:00 AM). Food and water was available ad libitum.

Rats were deeply anesthetized with an intraperitoneal injection of equithesin (mixture of 4.25 g of chloral hydrate, 2.13 g of $MgSO_4$, 16.2 ml of 6% pentobarbital sodium, 39.6 ml of propylene glycol, and 44.2 ml of water; initial dose: 3 ml/kg). A deep anesthetic plane, as determined by the depth and rate of the respiratory rhythm and an absence of the leg withdrawal reflex to a moderately intense toe pinch, was maintained for the duration of the experiment with supplemental doses of 0.2–0.3 ml every 20–30 min. Rectal temperature was maintained at 37 ± 0.5 °C by a homeothermic blanket (Harvard Apparatus, Holliston, MA), and

surgical wounds were regularly infiltrated with 2% procaine. The brain surfaces were kept moist with saline.

Electrophysiology

Recordings were performed on freely breathing rats. The animals were mounted into a stereotaxic apparatus. The dorsal surfaces of the MOBs were exposed through a hole drilled in the skull. The hole was extended caudally so that a stimulation electrode could be inserted into the lateral olfactory tract (LOT) through the overlying frontal cortex. The stimulation electrode, a concentric, bipolar, stainless steel electrode (Rhodes Medical Instruments, Summerland, CA), was positioned stereotaxically relative to bregma (2.3 mm anterior, 3.5 mm lateral, and between 7 and 7.5 mm deep, according to the atlas of Paxinos and Watson 1998). The depth was adjusted to optimize the amplitude of the large positive slow component of the field potential (FP), evoked by square wave stimulation of the LOT and recorded in the rostral–caudal, medial–lateral center of the MOB deep in the granule cell layer (depth = 1000 μm).

Extracellular unitary activities of mitral and tufted cells were recorded with glass micropipettes (10–15 MΩ) filled with 2 M NaCl saturated with pontamine sky blue. Unitary activities were amplified, band-pass filtered, and sent to a Cambridge Electronic Design (CED) 1401Plus system for off-line spike train analysis. The respiratory signal, recorded through a thermistor placed at the entrance of the nostril (Chaput and Holley 1979; Chaput et al. 1992), was sampled at 200 Hz and sent to the CED system.

The microelectrode was inserted into the dorsal surface and single-unit recordings were performed throughout the MOB. The laminar position of recorded cells relative to the MCL was determined during experiments by monitoring the dominant slow component of the FP (e.g., Phillips et al. 1963; Nickell and Shipley 1992). This FP component is negative when it is recorded from the surface of the MOB through the EPL, reverses polarity at the MCL, and is positive in the granule cell layer. The sequence of FP changes was also used to adjust the initial position of subsequent electrode penetrations. For example, if a penetration of the lateral bulb crossed the MCL to enter the granule layer within the first 800–1000 μm, the next penetration was positioned more laterally (or more medially) to increase the odds of recording from units in the EPL; with even more lateral (or medial) penetrations, we could sometimes record from units at the EPL–GB. Thus, many penetrations were more parallel to the layers of the bulb than perpendicular to them.

When possible, the position of the electrode tip was verified by marking the positions of the recording sites with small iontophoretic deposits of Pontamine sky blue (–10 μA current for 10 min, 10 s on, 10 s off). The location of the dye mark was evaluated in serial frozen section (40 μm thickness) of the MOBs stained with cresyl violet or neutral red. For Pontamine sky blue marked penetrations, electrode tracks were reconstructed from the position of these dye marks, the recorded depths, and the polarities and amplitudes of FPs evoked during each penetration (see Figure 1). Electrode tracks often exceeded 2000 μm from the bulb surface. During such a penetration, the FP could reverse polarity as the electrode first crossed the MCL could be positive for hundreds of microns while the electrode was in the granular cell layer and then reverse again to become negative as it traversed the EPL deeper in the bulb from its dorsal surface. Units were assigned to either the MCL or the EPL based on the polarity of the FP. The electrode track reconstructions based on dye marks support the accuracy of an identification of laminar position of recorded units based solely on FP data when no dye mark was recovered. For those units confirmed by track reconstructions, we could further subdivide the EPL units into those at the GB and those distributed deeper in the EPL. Units were identified as GB if the dye mark (maximum 25 μm diameter) touched the GB.

Experimental protocol

During the duration of the experimental protocol, rats were placed in front of an olfactometer which delivered a constant

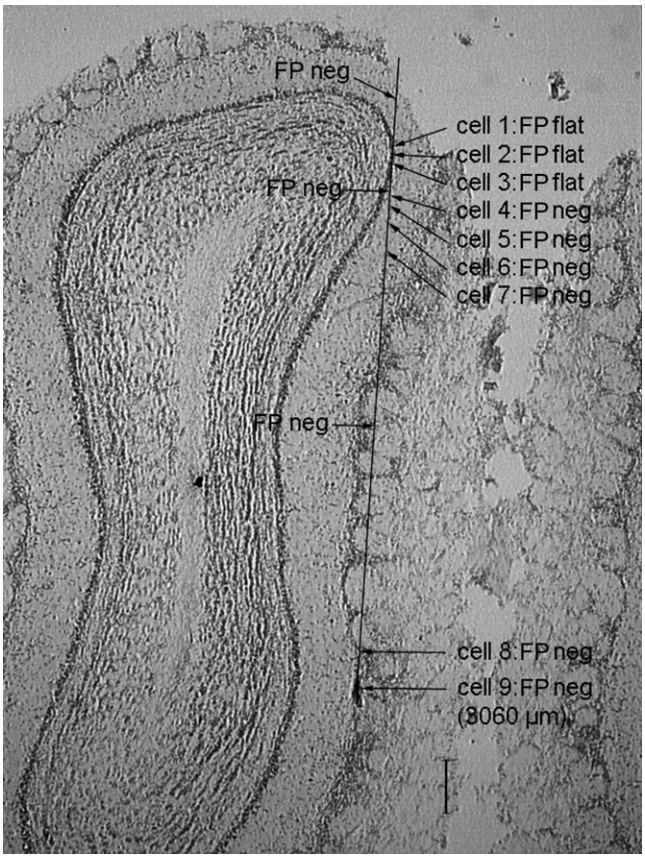

Figure 1 Electrode track reconstruction. The track was constructed based on a dye mark at depth 3060 μm and the polarity of the FP evoked by LOT stimulation (see text). Nine units were recorded during this penetration. The scale bar is 250 μm.

flow of deodorized and humidified air (30 l/min). For each unit encountered during an electrode penetration, we examined the amplitude and shape of the spontaneously generated action potentials (spikes) and the interspike intervals between these spikes (at least 2 ms) to insure single-unit recording. We also determined whether the unit could be driven antidromically from LOT with a constant latency, as measured on oscilloscope tracings, and, where possible, we recorded at least 10 antidromic action potentials for subsequent analysis of the latency. The stimulus for antidromic activation was a square wave pulse, 200–1000 μA (mean = 529 μA) in amplitude and 10–1000 μs (mean, 232 μs) in duration.

First, at least 180 s of spontaneous activity were recorded. Then, for many units, we were also able to record the responses to odor stimulation. Seven different pure chemical odorants were presented along with the odor of rat chow (2 times, once before and once after the chemical odorants). Odors were delivered during 10 s at more than 1-min intervals. In that later case, the 30 s of activity recorded just before each of the 9 odor presentations were processed as spontaneous activity. Results of these odor presentations are presented in the companion paper (Griff et al. 2008).

Data analysis

During experiments, signals were systematically stored for subsequent analysis on the 1 Gb SCSI hard disk of a computer connected to the CED-1401 Plus data acquisition system. Unit activity was digitized at 15 KHz to later extract spikes using the Spike2 software (CED). Each action potential in every record was examined to insure that the record was free of artifacts and that all action potentials were from a single unit.

Respiratory modulation of MOB spontaneous activity has been previously described in freely breathing animals; it produces bursting patterns of activity, most often with a firing increase during inspiration (Macrides and Chorover 1972; Chaput and Holley 1979; Chaput et al. 1992). Thus, some analyses of spike activity were performed with respect to the respiratory cycle by computer (modified CED Spike2 software). The respiration signal was first processed to discriminate respiratory cycles and to detect the transitions between exhalations and inhalations. The spike train was then displayed as cycle-triggered raster diagrams and cycle-triggered histograms (CTHs) aligned on the transition between inhalation and exhalation. The firing level of the cells was determined for the 180-s period of spontaneous activity sampled at the beginning of the recordings from the number of spikes in 100-ms bins, as done by Nagayama et al. (2004) and from the number of spikes per respiratory cycle. We also calculated the maximum and minimum levels per 100-ms bins and per respiratory cycle for each unit. These parameters were compared for the different cell types using a Student's *t*-test with the significance set at 0.05.

The firing activity during the 180-s period of spontaneous activity was also analyzed in terms of regularity, periodicity, and bursting. The degree of regularity of each cell was determined by calculating the coefficient of variation of its interspike intervals, that is, the ratio between the standard deviation (SD) and the mean of these intervals, build with a resolution of 5 ms and a time interval duration up to 2 s. To assess whether spike trains had oscillatory properties, that is, showed a pattern of neuronal activity in which discharges occurred periodically, we utilized the method described in detail by Kaneoke and Vitek (1996). This method detects the presence of multiple frequencies in cell autocorrelograms and evaluates the significance of frequencies detected. Autocorrelograms were constructed using a 5-ms time interval and 2 s of lag time and were smoothed by moving average method.

The periodicity in autocorrelograms was detected using the finite Fourier transform. Periodograms derived from these autocorrelograms were processed to get the significance of the frequency peaks detected against the null hypothesis that data had a white noise spectrum. Peaks detected with their *P* values less than 0.05 (Fisher–Kappa test) were considered to be significant and the corresponding spike trains were postulated to have oscillations at the frequencies detected. These analyzes were done using the SPECTRA procedure in the SAS software.

To detect the presence of bursts of action potentials, discharge density histograms using a bin size equal to the reciprocal of the mean discharge rate were constructed for each unit as described by Kaneoke and Vitek (1996). A Chi-square test with significance set at 0.05 determined whether each distribution followed a Poisson and the skew and kurtosis of each distribution were calculated. A Poisson distribution was expected if the discharge were random. If the spikes were regular and tonic, the distribution would not be Poisson or skewed but rather quasinormal. If the discharge contained bursts, the distribution would not be Poisson but would have a positive skew. Thus, spike trains were assumed to have burst periods when their discharge density histogram were significantly positively skew and different from a Poisson distribution with a mean of 1.0.

The synchronization of unit's firing activity with respiration was first analyzed using the CTH classification proposed by Chaput et al. in 1992 (Buonviso et al. 1992; Chaput et al. 1992) and extensively utilized by these authors in their subsequent publications. CTHs, which were subdivided into 45 bins, were grouped into 3 main classes, as shown as an inset in Figure 3. Whenever the units showed a uniform distribution of activity along the respiratory cycle, their patterns were classified as unsynchronized, and they were assigned to types 1a or 1b, according to whether the cells discharged a few occasional spikes or had a sustained firing activity. CTHs showing a single peak or trough of activity were classified as simple synchronized. They were classified as types 2a or 2b when excitation was superimposed on a low

background activity or on a sustained one and as type 3 when suppression occurred during a portion of the respiratory cycle. Lastly, complex activity patterns showing multiple activity changes along the respiratory cycle with respect to a mean level were classified as type 4a, 4b, 4c, or 4d, respectively, when histograms revealed a peak of excitation followed by a trough, a trough followed by a peak, a peak flanked by 2 troughs, or a trough flanked by 2 peaks.

CTHs were also utilized to analyze how the unit's activity was distributed along the respiratory cycle during the nine 30-s periods of spontaneous activity recorded before odor presentations. The bin firing rate for each histogram was calculated by averaging the bin firing in the 45 bins of the histogram. We also determined the minimum bin firing and the maximum bin firing in the 45 bins and calculated the firing range (maximum–minimum). We then calculated a mean bin firing rate for each unit by averaging the 9 individual histogram firing rates, and we did the same to obtain the mean minimum firing, the mean maximum firing, and the mean range.

When the distribution of the studied variable followed a normal law, a parametric analysis of variance (ANOVA) was done using general linear model procedures. Otherwise, 4 nonparametric tests were applied to the same variables, as usually done by statisticians. In situations where there was no significant change, using 4 tests increased our confidence in any observed lack of significant change. Indeed, finding several tests that rejected the null hypothesis that there was no significant difference is much more powerful than finding a single one (Feise 2002). The Wilcoxon rank sum test (Mann–Whitney U test) and the Van der Waerden test aimed to test the null hypothesis that the mean values of each variable were equal among the different cell types. The Kruskal–Wallis test, also called nonparametric ANOVA, is a generalization of the Wilcoxon. It was utilized to compare several modalities (data from different types of cells) in the same analysis, whereas the Wilcoxon test can compare only 2 modalities. The Kolmogorov–Smirnov test was also used; it examines whether the distribution of a variable is the same across different groups. These tests were applied using the UNIVARIATE and NPARWAY procedures in the SAS software. Their significance level was set to 0.05.

Discriminant analyses were done to determine whether there was a difference between the unit groups regarding the distribution of their firing activity along the 45 bins of the respiratory cycle, that is, their relationship with respiration. Thus, the goal of these analyzes was to find the bins that contributed the most to a good discrimination between the units. The method used was a discriminant factorial analysis, performed with the CANDISC and DISCRIM procedures in the SAS software.

This analysis was first performed on the MCL and EPL unit groups. There was thus 1 classification variable (cell type, a qualitative variable) and 45 quantitative variables (the firing frequencies in the 45 bins) identified by their rank. Factorial discriminant analysis was utilized to find: 1) a set of linear combinations of the quantitative variables that best revealed differences among the classes of units and 2) a subset of the quantitative variables that best revealed the differences among the cell types. Because the qualitative variable had only 2 modalities (MCL or EPL), the analysis gave only 1 discriminant variable, called Can1. After an examination of the scores of Can1, the variables (bins) corresponding to small scores in absolute values were removed until the error rate of classification by cross-validation was as small as possible (Lachenbruch and Mickey 1968; Lachenbruch 1979; Dillion and Goldstein 1984; Hand 1986). The analysis was repeated to determine which bins of the respiratory cycle best differentiate the respiratory synchronization of GB and not at the glomerular border (notGB) units. The qualitative variable was again the type of cell, but there are 3 modalities: MCL, GB, and notGB. Thus, the analysis calculated two discriminant variables Can1 and Can2. The data were again 60 observations and 45 quantitative variables identified by their rank. It was performed with the CANDISC and DISCRIM procedures in the SAS software.

Results

The results reported below are based on extracellular, single-unit recordings from the MOBs of 25 male Wistar rats. All units were antidromically activated from the LOT and therefore were classified as bulbar output neurons, namely, either mitral or tufted cells. Of the 1126 units that were isolated for at least a few minutes, 491 (43.6%) were antidromically driven from LOT; for many of these units, the antidromic action potential was only visualized transiently on the oscilloscope. In all, 635 units could not be antidromically activated, including 80 units where antidromic activation was not consistent.

Using the depth of the recording electrode in the bulb and the polarity of the dominant slow component of the FP evoked by LOT stimulation, we estimated the laminar position of these units in the MOB (see Materials and methods). Of the 491 antidromically driven units, 119 units were determined to have been recorded from the MCL and 263 units from the EPL based on the FP. In all, 109 units were excluded because the shape and/or amplitude of the FP did not allow a clear localization in the MCL or EPL. These 382 units (the 119 and 263 units recorded in the MCL and the EPL, respectively) were recorded throughout the MOB (57% were recorded from the medial bulb; 43% from the lateral bulb; average depth from the dorsal surface = 1655 μm). There was no significant difference between the average depths for MCL and EPL units.

For 80 of the 382 units, the laminar identification of the unit was strengthened by reconstructing the electrode track based on histological assessment of 1 or 2 dye markings. The depths of the electrode tip at the dye marks were used in conjunction with the FP data recorded during the penetration to

Table 1 Latency of antidromic action potentials

	All driven MCL	Confirmed MCL	All driven EPL	Confirmed EPL	Confirmed GB	Confirmed notGB
Number of units	119	19	263	61	14	47
Mean latency	2.61 ms	2.26 ms	2.64 ms	2.20 ms	1.99 ms	2.40 ms
SD	1.32	1.22	1.29	1.09	0.49	1.20

Antidromically driven units were labeled MCL or EPL based on the FP data. Confirmed units were classified based on electrode track reconstruction and antidromic activation that was repeated 10 times. See text for details.

reconstruct the track. Figure 1 shows a sample reconstruction. Thus, these 80 units were identified as mitral or tufted cells based on antidromic activation from LOT, the shape of the FP (reversing or negative), and the position of the tip of the recording electrode based on the track reconstructions. There were a total of 40 dye marks recovered, and in every case, the laminar position determined by the FP at that location agreed with the position of the dye mark.

Furthermore, for these 80 histologically confirmed units, repeated antidromic activations were recorded and we determined that the latency was constant for each unit. From the electrode track reconstructions, we were also able to confirm 19 units from the MCL and we were able to identify 14 units that were recorded from a portion of the EPL near the glomerular layer (GB) and 47 units from deeper in the EPL (notGB). The reconstructions also provide supportive evidence that the FP, when used in the absence of a dye mark and track reconstruction, provides an accurate measure for identifying the recording site.

Antidromic latency

In one of the first papers which describes tufted cells physiologically, Nicoll (1970) compared antidromic latency histograms from MCL and EPL units, and he concluded that they constitute 2 distinct populations. Table 1 shows antidromic latencies, measured from the time of LOT stimulation to the peak (or trough) of the antidromic action potential, for the different groups of units in the present study. Data from units of each group recorded from the medial, lateral, anterior, or posterior parts of the MOB were pooled because they were not significantly different. There was no significant difference between the mean latency of units recorded from the MCL and the EPL, whether we compared all driven units for each group or the histologically confirmed MCL and EPL units that had more accurate latency measurements (Student's *t*-test, either for equal or for unequal variances; significance level 0.05). By contrast, the mean latency of histologically confirmed GB units recorded from the EPL–GB was the shortest. It was statistically different from the mean latency of all MCL units (Student's *t*-test, for unequal variances; significance level 0.001), but it was not statistically different at 0.05 from the confirmed "notGB" units.

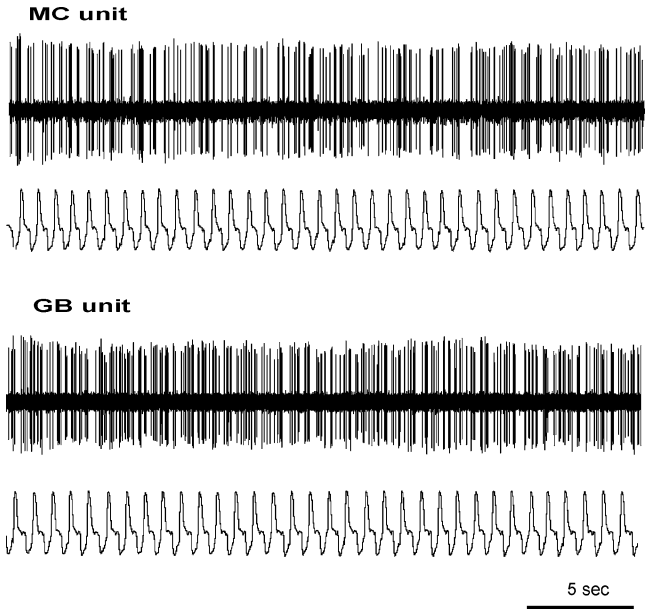

Figure 2 Examples of spontaneous firing activities recorded from a MCL unit (upper trace) and a GB unit (lower trace) in 2 different rats.

Mean spontaneous activity

The spontaneous activity of mitral and tufted cells was compared as done by Nagayama et al. in their 2004 paper to allow a direct comparison with our results. Of the 80 histologically identified cells above (where antidromic latency was compared), spontaneous activity was recorded for 47 units (14 MCL, 33 EPL of which 11 were GB and 22 notGB). To these, we added 38 units (25 MCL, 13 EPL–notGB) identified solely on the basis of FP recordings for a total of 85 units. These units exhibited constant latency, antidromic activation from LOT, and their spontaneous activity was recorded for at least 180 s. All units had a stationary firing activity (Dickey–Fuller test, 0.05 significance level; Dickey and Fuller 1979). Figure 2 presents an example of spontaneous firing activity of a MCL and a GB unit recorded in 2 different rats.

For each unit, we first calculated the maximum rate per 100-ms bin. Two other variables were also computed: the mean frequency (spikes per second) and the relative maximum rate per 100-ms bin (maximum rate per mean frequency (see Table 2). As shown by the Student's *t*-test, none of the

Table 2 Spontaneous activity: continuous recording

Variable	Cell types			
	MCL	EPL	notGB	GB
Mean frequency (Hz)	14.7 ± 6.2	16.6 ± 7.0	15.9 ± 6.4	18.9 ± 8.8
Max frequency (Hz; 100-ms bins)	75.0 ± 25.8	84.8 ± 33.7	79.4 ± 27.1	102.7 ± 47.3
Relative Max frequency (max frequency/mean frequency)	6.3 ± 6.4	5.4 ± 1.6	5.4 ± 1.8	5.5 ± 1.2

Several variables (left column) were calculated and compared for 39 MCL units and 46 EPL units consisting of 11 GB and 35 notGB. Values are means ± standard error.

differences between cell types (MCL vs. EPL, GB, or notGB units and between GB and notGB units) were significant at 0.05.

The spontaneous activity was also analyzed in terms of regularity, periodicity, and bursting. The different cell groups did not differ significantly in terms of regularity. No significant differences (Wilcoxon test, 0.05 significance level) were found between the groups, regarding mean interspike intervals and mean coefficients of variation. MCL, EPL, notGB, and GB units had, respectively, mean ± SD values of 0.0804 ± 0.0374, 0.0781 ± 0.0416, 0.0819 ± 0.0447, and 0.0634 ± 0.0210 s and mean ± SD of their coefficients of variations were 1.20 ± 0.36, 1.39 ± 0.54, 1.41 ± 0.57, and 1.32 ± 0.41. A second analysis aimed at determining whether the distribution of periodic and nonperiodic cells differ significantly between the different cell categories. Numbers of units having a periodic or a white noise firing activity did not differ significantly between the different cell groups (Chi-square test, 0.05 significance level). In all, 79.1% of the MCL, 81.3% of the EPL, 78.4% of the notGB, and 92.3% of the GB units showed a periodic activity. Thus, periodic activity or activity of white noise type did not depend on the cell type. Lastly, as shown in Table 3, the probability of observing a particular discharge type (not periodic and not bursting, periodic only, bursting only, periodic, and bursting) did not differ significantly between the cell groups (Chi-square test, 0.05 significance level). Thus, the type of activity did not depend on the cell type.

Table 3 Spontaneous activity: periodic and bursting cells

Cell type	Not periodic and not bursting	Periodic only	Bursting only	Periodic and bursting
MCL	9	0	22	12
EPL	12	2	31	19
notGB	11	2	22	16
GB	1	0	9	3

Numbers of not periodic and not bursting, periodic only, bursting only, and periodic and bursting cells in the different cell groups. These numbers did not differ significantly between the cell groups (Chi-square test, 0.05 significance level).

Respiratory CTHs

Numerous studies have shown that the MOB firing activity is modulated by respiration in freely breathing animals (Macrides and Chorover 1972; Chaput and Holley 1979; Chaput et al. 1992). The spontaneous activity of mitral and tufted cells was thus further analyzed by taking into account its relationship with respiratory activity. Eighteen MCL units and 42 EPL units of which 11 were GB and 31 notGB were included in this analysis. For each unit, we constructed 9 CTHs, 1 for each of the 30 s of activity recorded just before odor delivery during the 9 intervals inserted between odor presentations (see Materials and methods). Each CTH was divided into 45 bins and the number of spikes per bin tabulated. We calculated a mean bin firing rate for each unit by averaging the 9 individual histogram firing rates, and we did the same to obtain the mean minimum firing, the mean maximum firing, and the mean range. We also calculated the mean duration of the respiratory cycle for each recorded cell. Mean ± SD durations were 0.89 ± 0.11, 0.90 ± 0.14, 0.91 ± 0.16, and 0.90 ± 0.06 s for MCL, EPL, notGB, and GB units, respectively. They did not differ significantly (Wilcoxon test, 0.05 significance level). Thus, the results of the following analyzes could not be ascribed to differences in the duration of the respiratory cycle.

In order to get an overall indication of the level of firing of the units within the respiratory cycle, we calculated the mean, maximum, and relative maximum number of spikes per respiratory cycle. These 2 later values were reported because they cannot be predicted from the mean and depended strongly on the exact relationship of the cell firing activity with the respiratory activity. We also calculated the mean, minimum, and maximum bin firing rate for each histogram and the difference between the maximum and the minimum. Results from this analysis done on 60 observations from 60 units, corresponding to $60 \times 9 = 540$ CTHs, are shown in Table 4. Because the distribution of the variables did not follow a normal law, nonparametric statistical tests were applied (see Materials and methods). A significant difference at the 0.05% level was only found between MCL and GB units for 3 variables (mean bin firing with 3 tests, mean maximum and mean minimum bin firing with 1 test) and between GB

Table 4 Spontaneous activity: CTHs

Variable	MCL	notGB	GB
Mean number of spikes per respiratory cycle	10.7 ± 4.7	11.7 ± 4.7	14.0 ± 6.5
Max number of spikes per respiratory cycle	20.2 ± 7.5	23.1 ± 9.3	27.4 ± 15.0
Relative max number of spikes per respiratory cycle (max/mean)	3.7 ± 8.6	2.0 ± 0.4	1.9 ± 0.2
Mean bin firing	0.2165 ± 0.1114	0.2434 ± 0.1171	0.3382 ± 0.1320
Maximum bin firing	0.4396 ± 0.1958	0.5199 ± 0.2328	0.6944 ± 0.3723
Minimum bin firing	0.0552 ± 0.0529	0.06699 ± 0.0626	0.0907 ± 0.0314
Range	0.3844 ± 0.1753	0.4529 ± 0.2177	0.6038 ± 0.3692

Several variables (left column) were compared for 18 MCL units and 42 EPL units of which 11 were GB and 31 were notGB. Values are means ± standard error. They are in spikes per respiratory cycle (3 top rows) and in spikes per bin per respiratory cycle (3 bottom rows).

and notGB units for the mean bin firing with 1 test. No significant difference was found with the 4 tests between MCL and EPL units nor between MCL units and the notGB subgroup of EPL units for any of the other variables. Thus, GB units tended to have a higher spontaneous firing rate.

The subsequent analyses aimed at determining the impact of respiration on the firing activity of the different cell groups. They were performed on MCL and EPL units in an attempt to determine whether these 2 main categories of MOB output neurons showed firing differences and then on MCL, GB, and notGB units to examine possible differences within the EPL unit category.

The synchronization of unit's firing activity with respiration was first analyzed using the CTH classification shown as an inset in Figure 3. The distributions of the patterns of the different cell groups differed significantly (Table 5, Chi-square test, $P < 0.001$). The spontaneous activity of about 40% of the units was not synchronized with respiration (patterns 1a and 1b). As shown by comparisons between cell groups for each pattern made with the Fisher's Exact test (0.05 significance level), there was no significant difference in frequency between MCL and EPL (GB + notGB) units for these unsynchronized 1a and 1b patterns or for patterns displaying a simple synchronized increase in activity during the respiratory cycle (patterns 2a and 2b). However, a significantly smaller percentage of EPL units showed simple synchronized suppression in activity (pattern 3) and a significantly higher percentage showed complex patterns (4a–4d). The notGB units did not display significant differences with MCL units, except for 4a–4d patterns, whereas GB units showed a significantly lower frequency of 1a, 3, and 4a–4d patterns. Lastly, when compared with notGB units, GB units displayed a significantly lower proportion of 1a and 3 patterns and a higher proportion of 1b and 2b patterns. Thus, the different cell groups showed a differential modulation of their firing activity by respiration and the GB units displayed the most marked differences. More often, they had unsynchronized (type 1b) or simple synchronized (type 2b) high firing activities and less often had a low unsynchronized activity (type 1a) or a local inhibition (type 3).

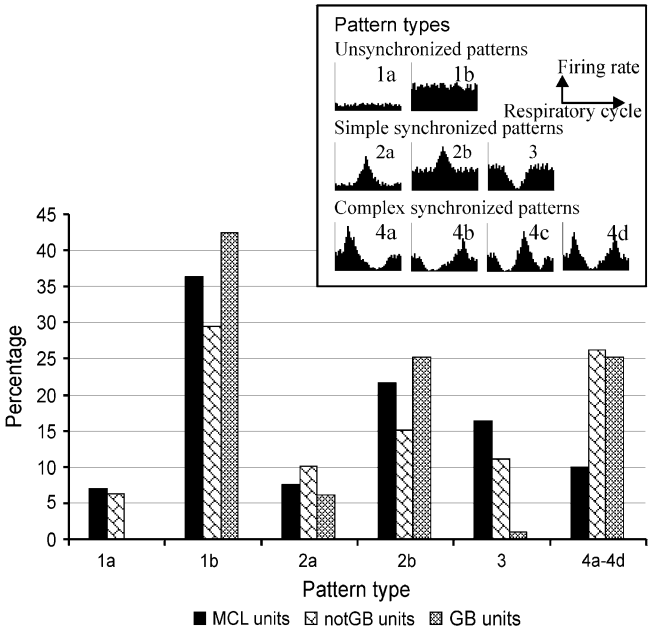

Figure 3 CTH types of spontaneous activity: The pattern types (1a–4d) are shown in the inset. The frequency (percentage) of pattern types for MCL, GB, and notGB units are compared. The distributions and then the proportions of each type in the different groups were compared using the Chi-square test. Significance levels are given in Table 5.

Discriminant analysis of MCL and EPL units

A first discriminant analysis (see Materials and methods) was performed to determine whether there was a global difference between the MCL and the EPL units in terms of the distribution of their firing activity during the respiratory cycle, before trying to determine whether there was a difference between MCL, notGB, and GB units. The goal of both analyses was to find the bins that contributed the most to a good

discrimination between the different units. In this first analysis, the qualitative variable had only 2 modalities (MCL or EPL) and gave only 1 discriminant variable, called Can1. An error rate of 0.1429, that is, 14% of misclassified units, was reached when 16 variables (bins) were retained, specifically, bins 2, 6, 7, 8, 10, 11, 13, 14, 19, 21, 24, 28, 30, 39, 40, and 45. The linear combination that best revealed differences between MCL and EPL units was

$$\begin{aligned}\text{Can1} = {} & 4.0936\,b_2 - 3.2799\,b_6 + 1.7796\,b_7 - 2.6566\,b_8 \\ & + 4.7945\,b_{10} - 4.2402\,b_{11} + 4.4633\,b_{13} - 3.1569\,b_{14} \\ & + 2.5949\,b_{19} - 4.4791\,b_{21} + 4.1611\,b_{24} - 4.7382\,b_{28} \\ & + 3.2243\,b_{30} - 3.1324\,b_{39} + 3.8364\,b_{40} - 3.0863\,b_{45},\end{aligned}$$

where b_i is the standardized firing activity in the bin i; the alternation of positive and negative signs in this equation was fortuitous. In the multidimensional space of the variables (the 16 bins), Can1 is the axis (the vector) that best discriminates MCL units from EPL units. This means that when the individual units (cells) are projected on this axis, the 2 classes of cells are well separated.

Figure 4A shows a representation of the units along the single canonical axis Can1; note that the procedure that calculates the canonical axis centers the distribution of points around zero. This discriminant axis opposes the 2 cell types, with all MCL units situated on the negative side of the axis and a majority of EPL units situated on the positive side of this axis. A few misclassified EPL units were found on the negative side confounded with the MCL units. By cross-validation analysis, all but one of these misclassified units were in the notGB group. Thus, MCL and EPL cell types may be assumed to form a continuum regarding this variable, with MCL units on one end and GB units on the other one.

Figure 4B shows how the activity in the 16 bins previously selected is distributed along the discriminant axis Can1. The coordinates of the variables (the activity in the 16 bins) are the coefficients of correlation between these variables and Can1. As visible in the figure, all bins were located on the positive side of Can1. They were thus positively correlated with Can1, which implies that units having the highest values on Can1 in Figure 4A had a high firing activity in these 16 bins. The highest correlation values were found for bins 13,

Table 5 Are they significant differences between the distributions into types and in the proportions of each type between 2 units groups?

		Unit types			
		EPL and MCL	notGB and MCL	GB and MCL	notGB and GB
Proportions of the 6 types		**S, P = 0.0002**	**S, P = 0.0006**	**S, P < 0.0001**	**S, P < 0.0001**
Histogram types	1a	NS (0.3119)	NS (0.8468)	**S (0.0106)**	**S (0.0109)**
	1b	NS (0.4391)	NS (0.1507)	NS (0.3659)	**S (0.0267)**
	2a	NS (0.6285)	NS (0.4110)	NS (0.6366)	NS (0.2358)
	2b	NS (0.2924)	NS (0.0788)	NS (0.5506)	**S (0.0333)**
	3	**S (0.0086)**	NS (0.1192)	**S (<0.0001)**	**S (0.0016)**
	4a–4d	**S (<0.0001)**	**S (<0.0001)**	**S (0.0015)**	NS (0.7947)

Chi-square test: S, significant at the 0.05 significance level; NS, not significant. The P values of the Fisher's Exact test are given in parentheses.

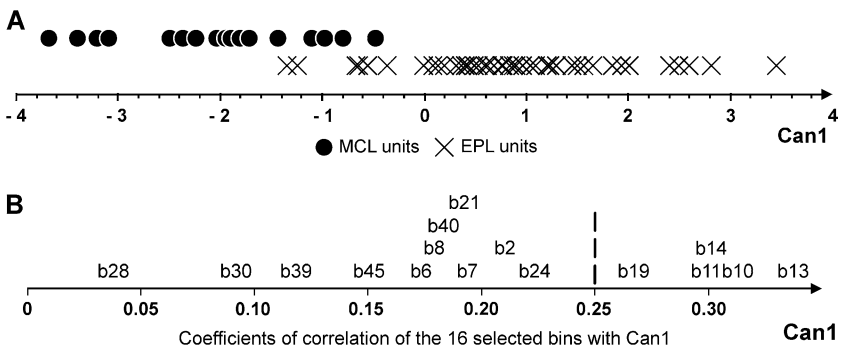

Figure 4 Discriminant analysis with 1 qualitative variable (cell type) and 2 modalities: Distribution of MCL (filled circles) versus EPL (×'s) units (in **A**) and of the coefficients of correlation of the 16 discriminant bins, b_i's, of the respiratory cycle (in **B**) along the first canonical axis, Can1. In both graphs, symbols or labels were displaced vertically to avoid overlapping. In B, all variables situated to the right of the dashed line have significant correlation coefficients with Can1.

14, 10, 11, and 19; these are bins (situated on the right side of the vertical line in Figure 4B) that correspond to the middle part of inspiration of the respiratory cycle. Thus, by using the position of the units on Can1 (Figure 4A) and the position of the bins on Can1 (Figure 4B), we conclude that the majority of the EPL units, which had positive values on Can1 in Figure 4A, had relatively high activity in the 16 bins and especially in bins 13, 14, 10, 11, and 19. On the other hand, MCL units, which had negative values on Can1 (Figure 4A), had a low activity in these 5 bins. Thus, the tufted cells were more active than the mitral cells during inspiration.

The distribution of Can1 for the different cells did not show a significant deviation from normality at the 5% level for the 4 tests usually applied by the UNIVARIATE procedure. Thus, it was possible to utilize an ANOVA on the variable Can1 to determine whether the difference shown above between mitral and tufted cells depended or not on the rat. As expected, a highly significant difference (F value = 78.68; P value < 0.0001) was found between MCL and EPL units because Can1 is the function that discriminates best between the 2 types of units. By contrast, no influence of the rat was observed (F value = 1.77; P value = 0.0793); thus, the spontaneous activity of a unit does not depend on the rat. Moreover, there was no interaction between the rat and the unit type (F value = 0.56; P value = 0.8213), which indicates that the difference between mitral and tufted cells observed with the discriminant analysis does not depend on the rat. In other words, no matter which rat is examined, the same difference between mitral and tufted cells will be found.

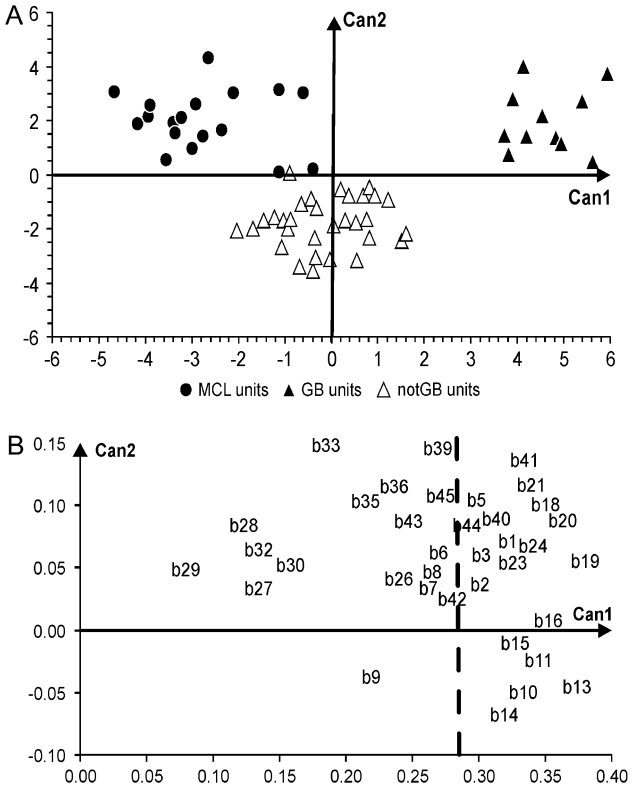

Figure 5 **A**) Discriminant analysis with 1 qualitative variable (cell type) and 3 modalities: MCL (filled circles) versus GB (filled triangles) versus notGB (open triangles) units: plot of first 2 discriminant axes, Can1 and Can2. (**B**). Distribution of bin activity along the 2 discriminant axes: The coefficients of correlation of the 36 discriminant bins are plotted on Can1 and Can2. Bins to the right of the dashed line are significant along the Can1 axis; bins 33, 39, and 41 are significant along the Can2 axis.

Discriminant analysis done on MCL, GB, and notGB units

Because the misclassified units on Can1 of the previous discriminant analysis were notGB cells, EPL units were suspected to form a heterogeneous population. In this second discriminant analysis, the qualitative variable had 3 modalities (MCL, GB, or notGB) and gave 2 discriminant variables, Can1 and Can2. Similar to the above analysis, 36 variables (bins) were retained to form 2 linear functions that discriminate best between the 3 types of cells. Here, an error rate of 0.1935, that is, 19% of misclassified units, was reached. The canonical correlation of the variable cell types with Can1 was equal to 0.94 and to 0.89 with Can2. Thus, the 2 axes discriminated well the 3 types of cells, as shown in Figure 5A. All the GB units have positive values on Can1, and all MCL units have negative values. Some notGB units, those situated on negative side of Can1, exhibited a firing behavior close to MCL units, that is, a relatively low activity during inspiration. By contrast, those notGB units situated on the positive side as GB units exhibited a relationship with respiration close to GB units with a relatively high firing activity during inspiration.

Figure 5B represents the activity in the 36 bins selected in the previous discriminant analysis; the coordinates for each bin are that bin's coefficients of correlation with the discriminant axes Can1 and Can2. The maximum of correlation with Can1 and Can2 was for bin19 (0.3747) and bin33 (0.1485), respectively. All the bins corresponding to inspiration (b1–b22) are situated at the most positive side of Can1 and are thus the most positively correlated with Can1. Thus, the GB cells, which have high values on Can1, have high firing activities in these bins, that is, during inspiration. By contrast, MCL cells, and to a lesser extent the notGB units, which have low values on Can1, have low firing frequencies during inspiration. On Can2, the activity in the bins 33, 39, and 41 is positively correlated with this axis. Thus, the MCL and GB cells, which are cells having the highest values on Can2, have the highest activity in these bins corresponding to expiration. By contrast, the notGB cells have the lowest firing activity in these bins.

Discussion

Mitral cells differ from tufted cells by the location of their cell bodies, the distribution of their lateral dendrites, and their cortical and subcortical projections. Though these

anatomical differences are well known, physiological differences between these neurons are less well understood. Only a single study has analyzed the spontaneous activity and the odor-evoked responses of these 2 categories of projection neurons, and this study was restricted to a localized zone of the MOB (Nagayama et al. 2004). The present paper compares the impulse conduction velocity and spontaneous activity of single units recorded in the MCL and in the EPL throughout the MOB. The overall conclusion is that the spontaneous activity and the impulse conduction velocity of mitral and tufted cells are similar, though some differences were found between mitral cells and tufted cells at the GB.

All units included in this study were reliably identified both as output neurons from the MOB and as units situated in the MCL, in the core of the EPL layer, or at its GB. The recording sites of all GB units were histologically confirmed. Some of the GB units are likely the cells referred to as superficial tufted cells (Ezeh et al. 1993) or superficially located middle tufted cells (Macrides and Schneider 1982). We chose not to use these designations because electrode track reconstructions and dye marks put some of the GB units deep in the glomerular layer at the EPL–GB. The GB units are also likely the same as the conventional projection type external tufted cells of Cajal (1911), which were based on the location of the soma; we chose not to use this name because this term is currently also used for external tufted cells that are not projection neurons (Kosaka K and Kosaka T 2005; Antal et al. 2006). The GB units in this paper are conventional projection tufted cells recorded in the superficial EPL at the GB that could be antidromically activated from the LOT. The decision to target GB cells and combine other tufted cells as notGB reflects in part our ability to identify GB cells as projection neurons recorded at the GB border and in part an interest in understanding the role of these neurons. In contrast, it is impossible to clearly distinguish MCL units from EPL units recorded in or near the MCL without intracellular recordings and dye filling of the cells because both are projection neurons (Schneider and Scott 1983).

The identification of many EPL and MCL units depended on the polarities or reversals of the FPs evoked by LOT stimulation recorded frequently during each electrode penetration. Shepherd and Haberly (1970) studied the topographical relationship between FPs and focal LOT stimulation and found that the polarity and/or reversal depth could change depending on the position of the LOT stimulation electrode relative to the recording site in the MOB due to nonuniform activation of the MOB. Nonuniform activation is unlikely a problem in the current experiments because relatively high stimulation currents were used and the electrode was positioned stereotaxically where LOT is relatively condensed (Paxinos and Watson 1998). Furthermore, 40 dye marks were recovered in these experiments, and the location of the electrode tip based on the polarity of the FP at the position where the dye was ejected always corresponded with the location of the dye mark. We cannot exclude the possibility that some of the units in the EPL were recorded from mitral cell dendrites, though the fairly large diameter of the recording electrodes and the stability of our recordings make this possibility less likely.

The latencies of both MCL and EPL units were the same (2.6 ms), though the latencies of GB units were shorter than MCL units. In these comparisons, no adjustments were made for the discrepancies in the distance between the stimulation and recording electrodes between units or between rats, but the maximum difference is likely less than 20% (2 mm anterior–posterior at bulb out of 10 mm from the MOB to the LOT stimulation electrode). In a paper on the MOB of rat, Scott (1981) has also compared units that could be antidromically activated only from the olfactory tubercle, units activated only from the piriform cortex, and units activated from both. Tubercle only units were recorded primarily from the EPL, whereas units activated from the cortex or from both the cortex and tubercle were recorded in or near the MCL. There were no significant differences between the latencies of these groups (1.7, 1.6, and 1.4 ms, respectively). However, in a paper on the MOB of rabbit, Nicoll (1970) presented a histogram of the latencies of EPL units with a mean of 14.9 ms and a range from 4.5 to 32.5 ms compared with MCL units with a mean of 2 ms and a range from 1 to 3.5 ms. He concluded that there are 2 distinct populations of cells based on antidromic latency, with EPL units having a much longer latency. The results reported by Nicoll may reflect a peculiarity of the rabbit.

The mean activity of EPL units (16.6 ± 7.0 Hz) found in the present study is not different from the value (16.9 ± 21.1 Hz) obtained by Nagayama et al. (2004), despite differences in the periods of activity taken as references and in the criteria for identifying EPL units. Indeed, we analyzed the spontaneous activity from periods of 180 s recorded before any stimulation while the rats were breathing clean air, whereas Nagayama et al. measured the spontaneous activity for 5-s period prior to recording responses evoked by odor stimulation. Furthermore, all the presumed tufted cells included in our calculation were antidromically activated, whether they were notGB or GB cells, whereas Nagayama et al. selected only the EPL units located between 50 and 250 μm from the flipover point in the MCL and rejected all the cells situated closer to the MCL or to the glomerular layer. Though not specifically addressed in the paper of Nagayama et al., these eliminated units situated near the glomerular layer appear to have a lower spontaneous activity, similar to the activity of mitral cells. As shown in Table 1, the units that we recorded at the GB units had, on the contrary, the highest spontaneous firing rates (18.8 ± 8.8 Hz). The mean activity of MCL units in the present study, 14.7 ± 6.2 is about twice that reported by Nagayama et al. (2004) (7.4 ± 6.6 Hz). This difference between the 2 studies could reflect differences in the anesthetic (urethane vs. equithesin) and/or the depth of anesthesia. If this explanation is correct, it would suggest that the spontaneous

activity of mitral and tufted cells is differentially sensitive to anesthesia.

In 1979, Chaput and Holley posited that synchrony between unit activity and the respiratory cycle was the most distinguishing temporal feature for cell classification. Almost 30 years later, the roles of temporal coding in transmitting olfactory information from the nose to the olfactory bulb to the cortex are still unclear. We, therefore, examined regularity, burstiness, and temporal oscillations in the spike discharges using a variety of approaches. The coefficient of variation of the interspike intervals has been used in a range of studies to characterize the regularity of spike discharge (e.g., Jones TA and Jones SM 2000). Bursting patterns can be detected by constructing density histograms of the intervals (Kaneoke and Vitek 1996) and the autocorrelation function has been used for decades to demonstrate periodicity in a spike train (e.g., Werner and Mountcastle 1963; Kozhevnikov and Fee 2007). None of these measures demonstrated any significant differences between mitral and tufted cells or between GB and notGB units.

The temporal relationship between spontaneous activity and respiration was first examined by comparing the patterns of CTHs (Figure 3). Because the duration of the respiratory cycle did not differ significantly between the different cell groups, differences in the proportion of the CTH types, as well as differences in mean firing activity discussed above, cannot be ascribed to differences in respiration. GB units exhibited significantly less simple suppression (pattern 3), possibly reflecting their smaller dendritic arborization. The greater activity of GB units and the lower frequency of the suppressive pattern may be ascribed to less influence of reciprocal inhibition compared with notGB or MCL units. Temporal relationships were further analyzed using a factorial discrimination analysis of the 45-bin respiratory cycle histograms to determine which bins produced the best discrimination between MCL and EPL units. The highest correlation values corresponded to the inspiratory part of the respiratory cycle and suggested that EPL units are more active than MCL units during inspiration. When the subclasses of EPL units are considered in a discrimination analysis, the results are more complicated. Some notGB units had low activity during inspiration, similar to mitral cells, whereas other notGB units had relatively higher activity during inspiration, similar to GB units. This could reflect the relatively high frequency of units with complex temporal patterns (Chaput et al. 1992) and indicate again that tufted cells form a heterogeneous population, as discussed extensively by Ezeh et al. (1993).

The relationship between spontaneous activity and respiration has been examined in only a few studies (for review, see Buonviso et al. 2005). Onoda and Mori (1980) examined activity changes induced by negative pressure pulses that pulled purified air across the nasal epithelia. The resultant airflow evoked an electro-olfactogram, and the authors could not eliminate the possibility that olfactory receptor neurons were responding to a contaminant, the odor of the animal itself, or the mechanical flow. Notwithstanding the possibility that the recorded activity is not truly spontaneous, the authors reported that only 14% of antidromically identified mitral cells exhibited distinct temporal patterning with respiration; this is in contrast to the 35% reported for mitral cells by Chaput et al. (1992). For the EPL units of Onoda and Mori (1980), a much larger percentage of EPL units exhibited temporal patterning. Because most EPL units in that study increased activity during inspiration (in-phase units), these results are consistent with our finding that EPL units are more active than MCL units during inspiration.

Several recent studies have examined neurons in the glomerular layer. An in vitro study by Hayar et al. (2004) recorded spontaneous activity from external tufted cells and reported that all exhibited spontaneous rhythmic bursts at 1–8 bursts per second. Periodic bursts at theta frequencies were not observed in the present study. Although the study of Hayar et al. included morphological reconstruction of the cell body and apical dendrites, reconstruction of the axon was truncated so that it was not possible to determine if these were projection neurons; not all neurons classified as external tufted cells project to the cortex via the LOT (for review, see Kosaka K and Kosaka T 2005). Although it is possible that the bursting cells of Hayar et al. (2004) are the same class of external tufted cells that were recorded in the present study, they do not seem to have the same morphology as the superficial tufted cells of Ezeh et al. (1993). The bursts observed in the in vitro preparation of Hayar et al. obviously could not have a relationship to respiration, though they concluded in their paper that a significant population of external tufted cells spontaneously generate rhythmic spike bursts at frequencies associated with rodent sniffing. However, we cannot discard the possibility that patterning with respiration could involve an entrainment of some endogenous bursting mechanism.

The conclusion from the present study is that EPL units and MCL units are similar in their impulse conduction velocity and in their spontaneous activity. However, there are several indications that GB units may be considered different in these characteristics. All GB units were identified by electrode track reconstructions; all were antidromically activated and the mean latency was shorter than either MCL units or notGB units. Using 3 nonparametric statistical analyses of respiratory CTHs, GB units had a higher mean bin firing than MCL units and 1 test indicated a higher firing than notGB units. Discriminant analysis indicated that GB units were more active during inspiration. The companion paper (Griff et al. 2008) shows that GB units are more active than MCL or notGB units during odor stimulation and the bins that contributed most to this discrimination occurred during inspiration. Because GB units could be antidromically activated from LOT, we consider them to be "conventional projection type external tufted cells" (Kosaka K and Kosaka T 2005). Additional

experiments, some of which are suggested in recent reviews of glomerular layer anatomy and physiology (Kosaka K and Kosaka T 2005; Wachowiak and Shipley 2006), will be needed to determine the roles of these external tufted cells in odor processing.

Funding

Centre National de la Recherche Scientifique Fellowship.

Acknowledgements

We would like to thank Florette Godinot for histology, Laure Marillet for her help on the statistical tests, and Patricia Duchamp-Viret for her helpful comments.

References

Antal M, Eyre M, Finklea B, Nusser Z. 2006. External tufted cells in the main olfactory bulb form two distinct subpopulations. Eur J Neurosci. 24: 1124–1136.

Berkowicz DA, Trombley PQ, Shepherd GM. 1994. Evidence for glutamate as the olfactory receptor cell neurotransmitter. J Neurophysiol. 7: 2557–2591.

Buonviso N, Amat C, Litaudon P. 2005. Respiratory modulation of olfactory neurons in the rodent brain. Chem Senses. 31:145–154.

Buonviso N, Chaput M, Berthommer F. 1992. Temporal pattern analyses in pairs of neighboring mitral cells. J Neurophysiol. 76:417–424.

Cajal LSR y. 1911. Histologie du Système Nerveux de l'Homme et des Vertébrés. Paris: Maloine.

Cant BB, Benson CG. 2003. Parallel auditory pathways: projection patterns of the different neuronal populations in the dorsal and ventral cochlear nuclei. Brain Res Bull. 60:457–474.

Chaput M, Holley H. 1979. Spontaneous activity of olfactory bulb neurons in awake rabbits, with some observations on the effects of pentobarbital anaesthesia. J Physiol (Paris). 75:939–948.

Chaput MA, Buonviso N, Berthommier F. 1992. Temporal patterns in spontaneous and odour-evoked mitral cell discharges recorded in anaesthetized freely breathing animals. Eur J Neurosci. 4:813–822.

Christie JM, Schoppa NE, Westbrook GL. 2001. Tufted cell dendrodendritic inhibition in the olfactory bulb is dependent on NMDA receptor activity. J Neurophysiol. 85:169–173.

Dickey DA, Fuller WA. 1979. Distribution of the estimators for autoregressive time series with a unit root. J Am Stat Assoc. 74:427–431.

Dillion W, Goldstein M. 1984. Multivariate analysis: methods and applications. New York: John Wiley & Sons, Inc.

Doving KB. 1987. Response properties of neurones in the rat olfactory bulb to various parameters of odour stimulation. Acta Physiol Scand. 130: 285–298.

Ennis M, Zimmer LA, Shipley MT. 1996. Olfactory nerve stimulation activates rat mitral cells via NMDA and non-NMDA receptors in vitro. Neuroreport. 7:989–992.

Ezeh PI, Wellis DP, Scott JW. 1993. Organization of inhibition in the rat olfactory bulb external plexiform layer. J Neurophysiol. 70:263–274.

Feise RJ. 2002. Do multiple outcome measures require p-value adjustment? BMC Med Res Methodol. 2:8.

Griff ER, Malhouz M, Chaput MA. 2008. Comparison of identified mitral and tufted cells in freely breathing rats: II Odor-evoked responses. Chem Senses. doi 101093/chemse/bjn040.

Haberly LB, Price J. 1977. The axonal projection patterns of the mitral and tufted cells of the olfactory bulb in the rat. Brain Res. 129:152–157.

Hand DJ. 1986. Recent advances in error rate estimation. Pattern Recognit Lett. 4:335–346.

Hayar A, Karnup S, Shipley MT, Ennis M. 2004. Olfactory bulb glomeruli: external tufted cells intrinsically burst at theta frequency and are entrained by patterned olfactory input. J Neurosci. 24:1190–1199.

Jones TA, Jones SM. 2000. Spontaneous activity in the statoacoustic ganglion of the chicken embryo. J Neurophysiol. 83:1452–1468.

Kaneoke Y, Vitek JL. 1996. Burst and oscillation as disparate neuronal properties. J Neurosci Methods. 68:211–223.

Kosaka K, Kosaka T. 2005. Synaptic organization of the glomerulus in the main olfactory bulb: compartments of the glomerulus and heterogeneity of the periglomerular cells. Anat Sci Int. 80:80–90.

Kozhevnikov AA, Fee MS. 2007. Singing-related activity of identified HVC neurons in the zebra finch. J Neurophysiol. 97:4271–4283.

Lachenbruch PA. 1979. Discriminant analysis. Biometrics. 35:69–85.

Lachenbruch PA, Mickey RM. 1968. Estimation of error rates in discriminant analysis. Technometrics. 10:1–11.

Macrides F, Chorover SL. 1972. Olfactory bulb units: activity correlated with inhalation cycles and odor quality. Science. 175:84–87.

Macrides F, Schneider SP. 1982. Laminar organization of mitral and tufted cells in the main olfactory bulb of the adult hamster. J Comp Neurol. 208:419–430.

Macrides F, Schoenfeld TA, Marchand JE, Clancy AB. 1985. Evidence for morphologically, neurochemically and functionally heterogeneous classes of mitral and tufted cells in the olfactory bulb. Chem Senses. 10:175–202.

Mori K, Kishi K, Ojima H. 1983. Distribution of dendrites of mitral, displaced mitral, tufted, and granule cells in the rabbit olfactory bulb. J Comp Neurol. 219:339–355.

Mouradian LE, Scott JW. 1988. Cytochrome oxidase staining marks dendritic zones of the rat olfactory bulb external plexiform layer. J Comp Neurol. 271:507–518.

Nagayama S, Takahashi YK, Yoshihara Y, Mori K. 2004. Mitral and tufted cells differ in the decoding manner of odor maps in the rat olfactory bulb. J Neurophysiol. 91:2532–2540.

Nickell WT, Shipley MT. 1992. Neurophysiology of the olfactory bulb. In: Serby MJ, Chobor KL, editors. The Science of olfaction. New York: Springer. p. 172–212.

Nicoll RA. 1970. Identification of tufted cells in the olfactory bulb. Nature. 227:623–625.

Onoda M, Mori M. 1980. Depth distribution of temporal firing patterns in olfactory bulb related to intake cycles. J Neurophysiol. 44:29–39.

Orona E, Rainer EC, Scott JW. 1984. Dendritic and axonal organization of mitral and tufted cells in the rat olfactory bulb. J Comp Neurol. 226:346–356.

Paxinos G, Watson C. 1998. The rat brain in stereotaxic coordinates, plate 10. San Diego (CA): Academic Press.

Phillips CG, Powell TPS, Shepherd GM. 1963. Responses of mitral cells to stimulation of the lateral olfactory tract in the rabbit. J Physiol. 168: 65–88.

Pinching AJ, Powell TPS. 1971. The neuron types of the glomerular layer of the olfactory bulb. J Cell Sci. 9:305–345.

Schiller PH. 1996. The On and Off channels of the mammalian visual system. Prog Retin Eye Res. 15:173–195.

Schneider SP, Scott JW. 1983. Orthodromic response properties of rat olfactory bulb mitral and tufted cells correlate with their projection patterns. J Neurophysiol. 50:358–378.

Scott JW. 1981. Electrophysiological identification of mitral and tufted cells and distributions of their axons in olfactory system of the rat. J Neurophysiol. 46:918–931.

Scott JW, Harrison TA. 1987. The olfactory bulb: anatomy and physiology. In: Finger TE, Silver WL, editors. Neurobiology of taste and smell. New York: Wiley. p. 151–178.

Shepherd GM, Haberly LB. 1970. Partial activation of olfactory bulb: analysis of field potentials and topographical relation between bulb and lateral olfactory tract. J Neurophysiol. 33:645–653.

Stewards TV, Stewards M. 2002. Separate, parallel sensory and hedonic pathways in the mammalian somatosensory system. Brain Res Bull. 58:243–260.

Wachowiak M, Shipley MT. 2006. Coding and synaptic processing of sensory information in the glomerular layer of the olfactory bulb. Semin Cell Dev Biol. 17:411–423.

Werner G, Mountcastle VB. 1963. The variability of central neural activity in a sensory system, and its implications for the central reflection of sensory events. J Neurophysiol. 26:958–977.

Accepted June 17, 2008